Int. J. Electrochem. Sci., 12 **(2017)** 1348 – 1361, doi: 10.20964/2017.02.04

International Journal of
ELECTROCHEMICAL
SCIENCE
www.electrochemsci.org

Effect of Passivation Potential on Passive Behavior and Corrosion Resistance of Ni-Cu-P Amorphous Coating in Alkaline Solution

Jie Chen[1], *Yong Zou*[1,*], *Kenji Matsuda*[2], *Guanlin Zhao*[1]

[1] Key Lab of Liquid Structure and Heredity of Materials, Ministry of Education, Shandong University, Jinan 250061, Shandong, China.
[2] Department of Materials Science and Technology, Faculty of Engineering, University of Toyama, Toyama, 930-8555, Japan.
[*]E-mail: yzou@sdu.edu.cn

Received: 23 October 2016 / *Accepted:* 12 December 2016 / *Published:* 30 December 2016

Corrosion resistance and passive behavior of electroless Ni–Cu–P amorphous coating have been investigated in 10 wt.% NaOH solution by using electrochemical impedance spectroscopy, Mott–Schottky and X–ray photoelectron spectroscopy analysis. The result that the corrosion resistance is increased firstly and then exhibits an opposite trend with the increasing passive potential is resulted from the variation of passive film on the coating. Passive films formed at lower potential possess n–type and p–type bipolar semiconductors characteristics, but the passive films formed at higher potential have only p–type semiconductor characteristics. The thickness of passive films was increased with the increase of passive potential. The corrosion resistance of passivation films is combined affected by their thickness and their semiconductor type.

Keywords: Ni–Cu–P; Amorphous coating; Corrosion resistance; Passive films; XPS

1. INTRODUCTION

Electroless Ni–based amorphous coatings, including Ni–Cu–P, are widely used because of their excellent corrosion resistance [1-6]. It is generally accepted that the high corrosion resistance of amorphous Ni–based alloys is attributed to the suppression of their anodic dissolution, the so-called passivation film theory. Passivity is defined as a decrease in the corrosion rate of a metal or alloy by forming a thin and tenacious protective film [7].

The properties of a passive film like thickness, semiconductor type, and composition have great influence on the protectiveness of a passive film, which is affected by external factors. One of them is the formation potential, which affects the properties of a passive film a lot and is a key role in the protective barrier to corrosion. According to the Point Defect Model (PDM), the thickness of the barrier layer increases linearly with formation potential for the cases where no change in the oxidation state occurs [8-10]. Rossi et al. [11] studied the passive film of a Fe-based amorphous alloy and concluded that the thickness of the film increases with the increasing film formation potential. Semiconducting properties of passive films are usually studied by Mott–Schottky (M–S). The donor/accepter density and semiconductor type changes with the variation of film formation potential [7, 12]. Passive films possessing a bipolar characteristic show the best corrosion resistance by obstructing the positive ions out as well as resisting the negative ions in [13-15]. The compositions of passive films are usually studied by X–ray photoelectron spectroscopy (XPS). Lee et al. [16] studied the passive film of Zr–4 alloy and discovered that the film contained a hydrous ZrO_2 layer at lower potential, but, it was made up of duplex layers (an outer hydrous ZrO_2 layer and an inner anhydrous ZrO_2 layer) at higher potential.

Previous studies on the passive film of Ni–based amorphous coatings mainly focused on the chemical composition and surface morphology [17]. Investigations on the semiconductor properties of passive film are limited, which is the most direct reflection of its physical and chemical structure. Ni–Cu–P is one of the Ni–based amorphous coatings with better corrosion resistance than others [18-20]. Thus, this work aims at giving insight into the effect of applied potential on passivation and corrosion resistance of Ni–Cu–P amorphous coating in 10 wt.% NaOH solution. Passive films with different formation potential were prepared by potentiostatic polarization experiments. Corrosion resistance and passive behavior of the films were studied via electrochemical impedance spectroscopy (EIS), M–S and XPS analysis.

2. EXPERIMENTAL

2.1. Preparation of Ni–Cu–P electroless coating

The substrates were Q235 sheets with a size of 10 mm × 10 mm × 1 mm. Before plating, the substrates were polished and cleaned thoroughly. In electroless plating solution, nickel sulfate and copper sulfate are the sources of Ni and Cu, the sodium hypophosphite is a reducing agent. Sodium citrate serves as complexing agent, and the glycine and anhydrous sodium acetate acts as stabilizers. Plating was conducted in a constant temperature water bath at 82–88 °C for 3 h, and the PH value is about 4.7.

2.2. TEM test

Morphology and structure of Ni–Cu–P electroless coating are studied by TEM (JEM–2100). The work voltage is 200 kV. The TEM samples are prepared by Twin Jet Thinning instrument, and the

work current is 30–50 mA. The electrolyte is the mixture of perchloric acid and methanol with the proportion of 1:9.

2.3. Electrochemical measurements

The electroless Ni–Cu–P coating is passivated by potentiostatic polarization of an autolab electrochemical workstation (Aut84886). Five different film formation potentials were selected from the stable passive region, and then the coatings were passivated in etching solution (10 wt.% NaOH) for 3600 s respectively.

The electrochemical test system is the classic three-electrode system with a platinum plate as counter electrode, an Ag/AgCl as the reference electrode and the sample as the working electrode. The passive region was obtained from the polarization curves of the Ni–Cu–P coating. The scanning range of polarization is -0.3 – 1 V (relative to the open circuit potential) and the scan rate are 0.5 mV/s.

The corrosion resistance of the passive Ni–Cu–P coatings is analyzed by EIS. The impedance scanning frequency is 100,000 – 0.01 HZ and the amplitude is 10 mV. Semiconductor type and the donor/acceptor densities of the passive films were calculated from Mott–Schottky (M–S) curves. M–S plots were obtained by performing a potential scan from –0.5 V (vs. SCE) to 0.5 V (vs. SCE) at a 1000 HZ fixed frequency. Each test was repeated at least thrice to ensure the reproducibility of the results.

2.4. XPS analysis

The composition of the passivation film formed on Ni–Cu–P coatings is studied by XPS (ESCALAB 250). The working environment is Al Kα, 15 kV and 150 W, and the scanning angle is 45°. The scanning range of the normalized XPS survey is 0–1050 eV. High resolution XPS spectrums were extracted to study the differences of each element. In order to compensate for the charge shift during the photoelectron ejection process all spectra were corrected by referencing to the C 1s spectra at 284.6 eV. The peak assignments are based on a comparison with spectra recorded from known nickel, copper and phosphorus compounds.

3. RESULTS AND DISCUSSION

3.1. Morphology and microstructure analysis of Ni–Cu–P coating

The morphology of the plating is shown in Figure 1. SEM observation shows that this Ni–Cu–P coating presents a spherical nodular feature and is relatively homogeneous. The diameter of the nodules is below 10 μm. The macroscopic cross profile of the coating was inserted in the upper right corner of Fig. 1. It can be seen clearly that the thickness of the coating is about 30 μm. The thicker layer helps reduce porosity in the as-plated Ni–Cu–P coating, thus inhibiting the corrosion reaction between the through pores and substrate. TEM observation results indicated an amorphous structure of the coating (Fig. 2), as the bright field image of the coating is featureless, and the selected area electron

diffraction patterns (SADP) for specimen is showing a halo ring rather than diffraction dots. EDS analysis indicated that the content of the as–deposited coating is Ni–2at.%Cu–23at.% P.

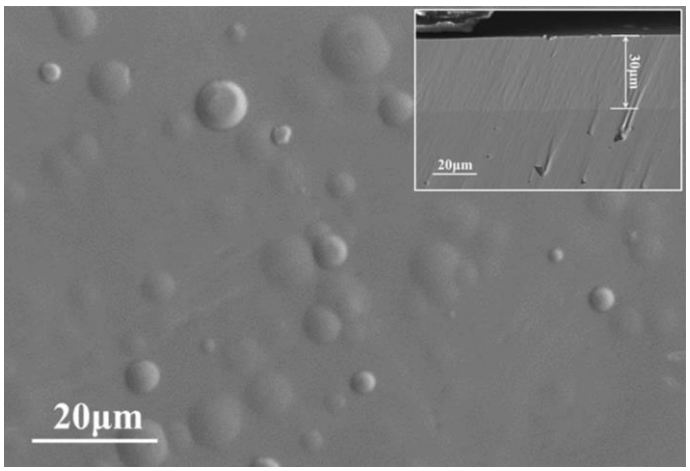

Figure 1. SEM results of as–deposited Ni–Cu–P coating.

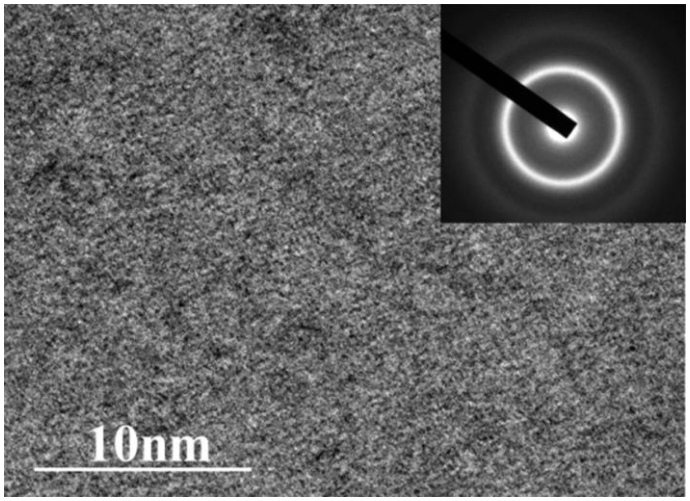

Figure 2. TEM results of as–deposited Ni–Cu–P coating.

3.2. Polarization curves analysis

The polarization characteristic of the Ni–Cu–P plating in 10 wt.% NaOH solution was evaluated by potentiodynamic polarization technique as illustrated in Figure 3. The polarization curve indicates the coating having obvious passivation behavior, and the stable passivation range is from –0.3 to 0.1 V. According to the dissolution-precipitation mechanism of $Ni(OH)_2$ passivation film [21], the active region of the anodic polarization curve is considered to be Ni dissolution. The current decrease at higher potential is due to the formation of $Ni(OH)_2$ and attainment of a stable passive region. When the potential increases to a certain degree, the oxidation of $Ni(OH)_2$ to NiOOH may occur and the passive film begins to be destroyed. To study the effect of passive potential on corrosion

resistance of the electroless Ni–Cu–P coating, five different passivation films were prepared by potentiostatic polarization at the film formation potential of –0.3, –0.2, –0.1, 0, and 0.1 V respectively. The passivation time is 3600 s.

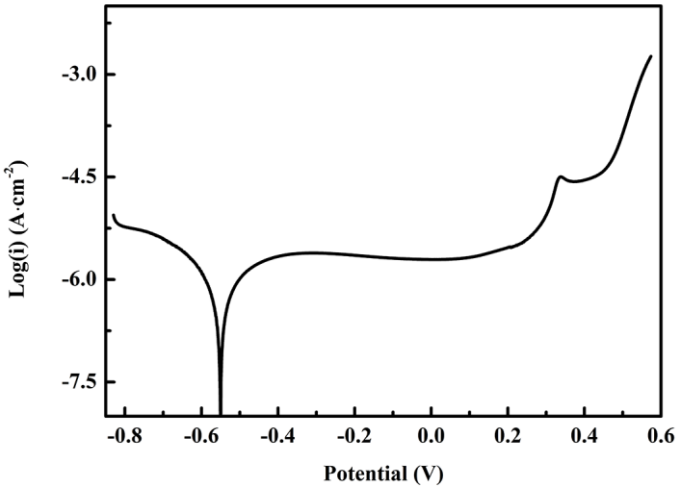

Figure 3. The polarization curve of Ni–Cu–P electroless plating in 10 wt.% NaOH solution.

3.3. EIS analysis

The corrosion resistance of the as–deposited coating and five different passivated coatings are measured by EIS, which were conducted at open circuit potential, and the results are shown in Figure 4 and 5. As seen in Fig. 5 (a), the deposited coating display only one broad maximum phase lag and phase lags approach zero if the test frequency is near 10^5 and 10^{-2} Hz. It implies that only one capacitive response exists. So, the as–deposited coating has one time constant in the corrosion process, corresponding to the solution and Ni–Cu–P coating interface. However, in Fig. 5 (b), the frequency vs. phase curves of passivated coatings showed two peaks of phase lag, indicating two time constants in the corrosion process, corresponding to the solution/passive film interface and solution/as-deposited coating interface. The equivalent circuit of $R_s(C_{dl}R_{ct})$ was chosen for the as–deposited coating, and $R_s(Q_f(R_f(C_{dl}R_{ct})))$ for the passivated coatings to fit the EIS results. In the circuits, R_s is solution resistance, Q_f is the constant–phase element (CPE) of passive films, R_f is the passive film resistance, C_{dl} is the double–layer capacitance and R_{ct} is the charge transfer resistance. The CPE was used as the non-ideal capacitance ($n < 1$) of the passive film caused by surface heterogeneities and toughness, as given by $Z_{CPE} = [Q(jw)^n]^{-1}$, where Q is the admittance of CPE, n is the CPE exponent, and w is the angular speed. The higher value of R_{ct} indicates better corrosion resistance, thus it can be used to evaluate the corrosion resistance of the samples. Table 1 is the parameters' values calculated from the EIS results.

From Table 1, it can be discovered that the R_{ct} of as–deposited coating is much smaller than that of the passivated coatings. This indicated that the coating passivated in the air was less corrosion resistant than that after potentiostatic polarization in 10 wt.% NaOH solution. In general, the corrosion resistance of the coatings increases firstly and then shows the opposite trend with the increase of passive film formation potential. The coating passivated at –0.1 V shows the best corrosion resistance.

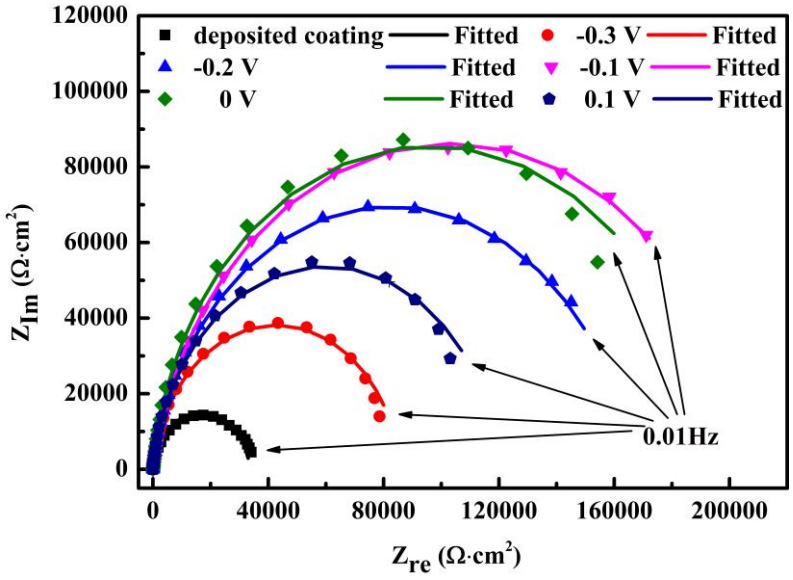

Figure 4. Nyquist plots of as–deposited and passivated Ni–Cu–P coatings in 10 wt.% NaOH solution.

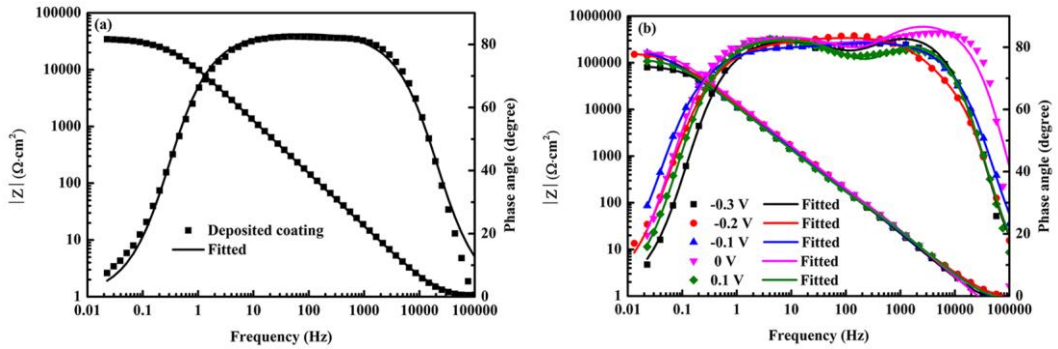

Figure 5. Bode spectrums of (a) as–deposited coating, and (b) passivated coatings in 10 wt.% NaOH NaOH solution.

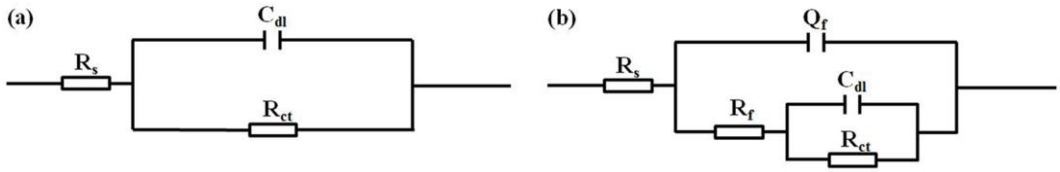

Figure 6. The equivalent circuits of: (a) $R_s(C_{dl}R_{ct})$ and (b) $R_s(Q_f(R_f(C_{dl}R_{ct})))$.

Table 1. EIS fitting results of as–deposited and passivated coatings.

	As-deposited	-0.3 V	-0.2 V	-0.1 V	0 V	0.1 V
R_s	1.0	0.723	0.956	0.641	0.291	0.816
R_{ct}	3.36E+04	8.58E+04	6.60E+04	2.09E+05	1.95E+05	1.20E+05
R_{coat}	\	463.7	528.4	675.5	319.7	257.9

3.4. M–S analysis

Figure 7 shows M–S plots of coatings passivated with different passive film formation potential. The linear segment of M–S curve represents the depletion of majority–carriers in the space–charge layer. When the M–S curves emergence more than one linear segment, there exists not only one space–charge layer. The changed orientation of the M–S curve is the result of the series–wound system of the space–charge layers [22]. In Fig. 7, the M–S curves of passive films at –0.1, 0 and 0.1 V represent a linear segment at the potential range of –0.4 and 0.4 V indicating only one space–charge layer. The negative slopes indicate the p–type semiconductor of passive films, but the slopes are different. However, for the samples passivated at –0.3 and –0.2 V, the M–S curves represent two linear segments, which is the n–type space–charge layer at lower potential range (–0.4 to 0 V) and p–type space–charge layer at higher potential range (0 to 0.4 V). In the low potential region, p–type semiconductor is an accumulation state, and the n–type semiconductor is a depletion state. Due to the capacitance of the accumulation state is much larger than that of the depletion state. The results of these two series–wound space–charge layers make the total capacitance show the p–type semiconductor characteristics. And when the potential rises, p–type semiconductor will be exhausted from the accumulation state, while the n–type semiconductor change from the depletion state to the accumulation state, then the total capacitance presents an n–type semiconductor characteristics. This passive film with two space–charge layers is often regarded as a bipolar semiconductor passive film.

The different semiconductor property of passive films at different passive potential is probably caused by the changes in the compositions and structures. Different oxide layers formed in alloys exhibit different semiconducting properties according to the main defects in the films [23]. Element P is usually regarded as n–type semiconductor by anion diffusion into the metal or by cation transport through interstitial diffusion [24, 25]. While oxides like NiO_2, NiO and Cu_2O are considered as p–type semiconductor for their properties with a deficiency in metal ions or excess with cation vacancies [26-28]. In consequence, it is reasonable to draw an inference that the main oxides of the passive film on Ni–Cu–P coating change with the increasing passive potential.

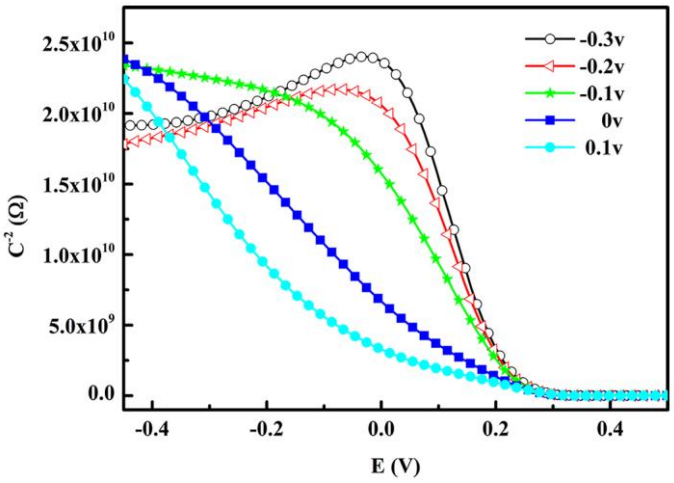

Figure 7. Mott–Schottky curves of passivation films.

3.5. XPS analysis

The composition and structure of passive films greatly affect their anti-corrosive property. The differences of oxides of the elements in the passive film should be investigated to understand the effect of passive potential on the corrosion resistance of passive films. Through the EIS and M–S results, it can be discovered that the passive film formed at –0.1 V has the best corrosion resistance. So, XPS curves of passive films are analyzed, which were prepared at –0.3, –0.1 and 0.1 V in 10 wt.% NaOH for 3600 s. For comparison, the binding energies of some known nickel oxide, copper oxide and phosphorus compounds are listed in Table 2.

Table 2. Ni 2p3/2, Cu 2p, P 2p and O 1s binding energy for known Ni, Cu and P compounds

Element	Spectral line	Compound	Energy (eV)	Ref.
Ni	2p3/2	Ni^0	853.0	[29]
Ni	2p3/2	$Ni(OH)_2$	855.78	[30]
Ni	2p3/2	NiO	856.5	[31]
Cu	2p3/2	$Cu(OH)_2$	932.7	[32]
Cu	2p3/2	Cu_2O	932.0	[33]
Cu	2p3/2	CuO	933.3	[34]
P	2p3/2	P^0	129.7	[21]
O	1s	$Ni(OH)_2$	531.7	[35]

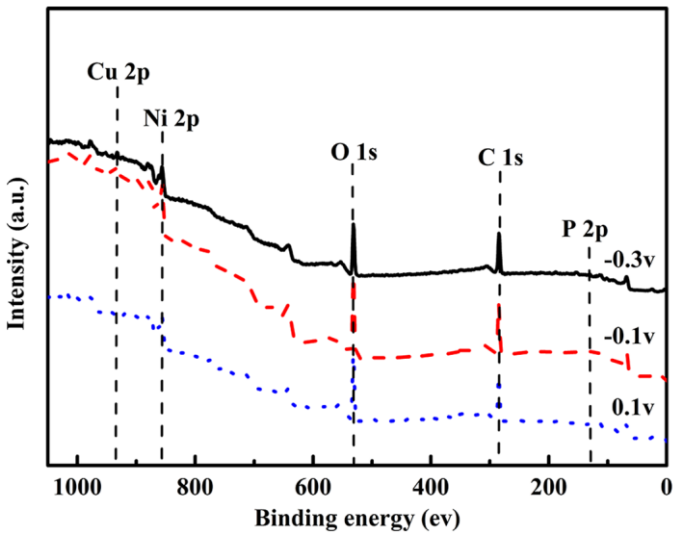

Figure 8. The normalized XPS spectrum for Ni–Cu–P electroless coating polarized at –0.3, –0.1 and 0.1V in 10 wt.% NaOH solution.

Figure 8 shows the normalized XPS spectrums of the three passive films. Some positions of reference spectra are marked with dashed lines and the elements are marked in the corresponding location. These curves are almost same, mainly composed of Cu, Ni, O, C and P. Surface oxidation and contamination in the form of adsorbed gas species accounted for the O_2 and C [36]. However, the position and intensity of the strongest peak of each element are slightly different. So, high resolution XPS spectrums (Fig. 9) of the main elements are analyzed to identify the difference, which is mainly affected by passive potential.

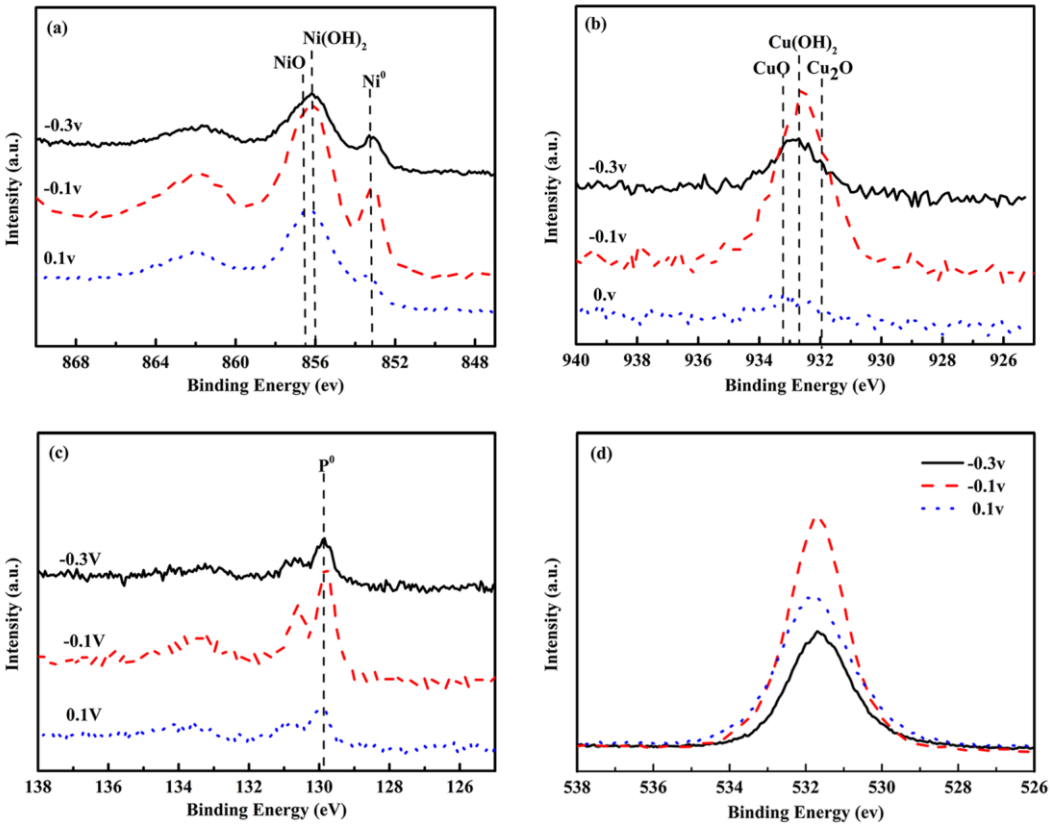

Figure 9. XPS spectrums of (a) Cu 2P, (b) Ni 2P, (c) P 2P and (d) O1S for Ni–Cu–P electroless coating polarized at –03, –0.1 and 0.1V after 3600s in 10 wt.% NaOH solution.

Figure 9(a) is the spectrums of Ni 2p3/2. For passive films formed at –0.3 and –0.1 V, the center of the Ni 2p3/2 spectrum is located at 855.78±0.2 eV, confirming the presence of $Ni(OH)_2$ (855.78 eV) as the main composition in the passive film. There are also some NiO (856.5 eV) and Ni^0 (853.0 eV) for the change of the curve in the corresponding positions. However, the passive film formed at 0.1 V, the center of the Ni 2p3/2 spectrum shifts to higher binding energy (856.4 eV). Ni^0 was detected on all samples, indicating the thickness of the passive layer was less than the XPS sampling depth for Ni.

The peaks of Cu 2p are shown in Figure 9(b). The main composition for the film formed at –0.3 V is $Cu(OH)_2$ (932.7 eV), followed by Cu_2O (932.0 eV) and CuO (933.3 eV). The passive film formed at –0.1 V, the center of the Ni 2p3/2 spectrum shifts to lower binding energy (932.0 eV). The intensity

of the curve at 0.1 V is not strong, but some undulations can be distinguished. The center of the Cu 2p spectrum locates at 933.3 eV.

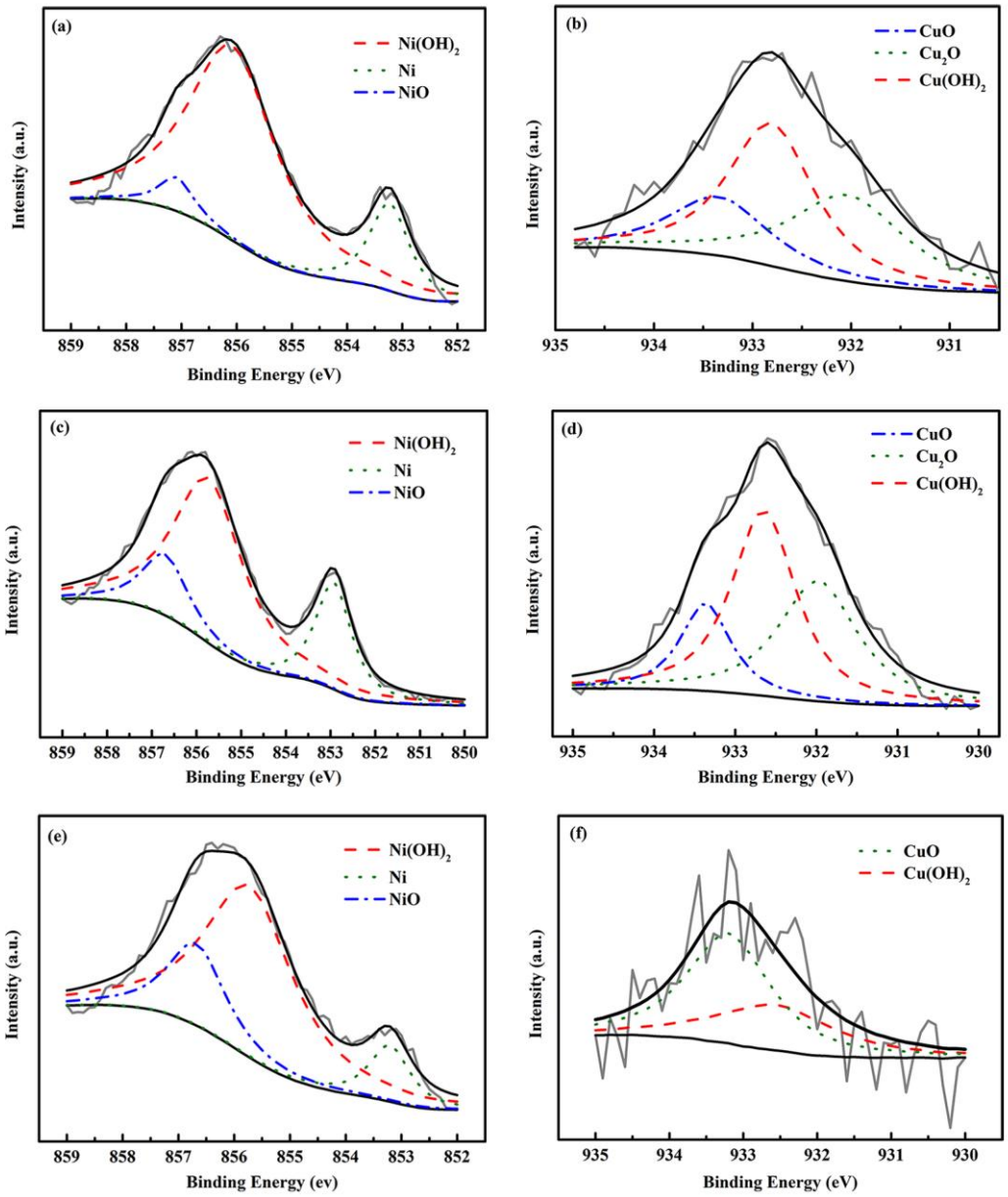

Figure 10. The detailed XPS spectra of Ni 2p 3/2 and Cu 2p 3/2 of the passive films formed on amorphous Ni–Cu–P coating, which were passivated at: (a) –0.3 V, (b) –0.3 V, (c) –0.1 V, (d) –0.1 V, (e) 0.1 V, (f) 0.1 V after 3600 s in 10 wt.% NaOH solution.

Figure 9(c) is the spectrums of P 2p. Three passive films formed at –0.3, –0.1 and 0.1 V are all composed of P (129.7 eV). PO_4^{3-} had been detected in as-deposited Ni–P alloys and the alloys exposed to acid sulfate and chloride environments [21, 36, 37]. But, XPS data showed no PO_4^{3-} on the surface after polarized in 10% NaOH. This is because $Ni_3(PO_4)_2$ with higher solubility than NiO and $Ni_3(PO_4)_2$ is 2 to 3 orders of magnitude more soluble in slightly alkaline solutions than $Ni(OH)_2$ (in mol/kg water: $Ni(OH)_2$ =1×10^{-7} to 7×10^{-6}; $Ni_3(PO_4)_2$= 2.5×10^{-4}) [36]. XPS data also showed no P-O compounds on the surface of the passive films, which indicated that the detected P^o was related to the bulk alloy or to

an intermediate P–enriched (or depleted) layer. The O ls spectrum (Figure 9 (d)) exhibits a broad signal which is mainly composed of a large amount of $Ni(OH)_2$ and some other oxides and hydroxides.

The spectra of Ni 2p and Cu 2p was taken out to conduct a deep study because it was not easy to point out the main oxidation states of Ni and Cu in some passive potential from Figure 9. After background subtraction, the XPS results were separated into contributions of different oxidation states as shown in Fig. 10. Fractions of Ni, Cu, P and O in the passive films were figured out and presented in Fig. 11. Besides, fractions of Ni oxides as well as the Ni^{2+}/Ni^0 ratio were figured out and shown in Table 3.

From Table 3, it is apparent that the fractions of $Ni(OH)_2$ is greater than NiO and Ni^0, so the passive films are mainly composed of $Ni(OH)_2$, which is also the primary constituent of passive films formed on Ni-P surface in alkaline solution [21]. This is because the amount of Cu in the coating is only 2 at.% in this study, which may be dissolute in the Ni lattices [38]. Thus, the Ni remains the major element in Ni–Cu–P coating. In addition, samples polarized at –0.3 and –0.1V shows a low Ni^{2+}/Ni^0 ratio, while the coating polarized at 0.1V had a higher ratio. A higher Ni^{2+}/Ni^0 ratio indicated a thicker $Ni(OH)_2$ film. The thickness of the $Ni(OH)_2$/NiO layer was increased with the increase of passive potential.

In Figure 11, it is obvious that Ni is the main element in the passive film except for O, followed by P and Cu. Besides, the content of P is decreased with the increase of passive potential. The formula of P is P^0, which was related to the bulk alloy. The XPS results suggested the thickness of passive films on the amorphous Ni–Cu–P coating was increased with the increase of the applied potential. This dependency relationship between the thickness of the barrier layer and the passive potential have also been reported in previous studies [23, 39], which is in line with the theory of Point Defect Model (PDM).

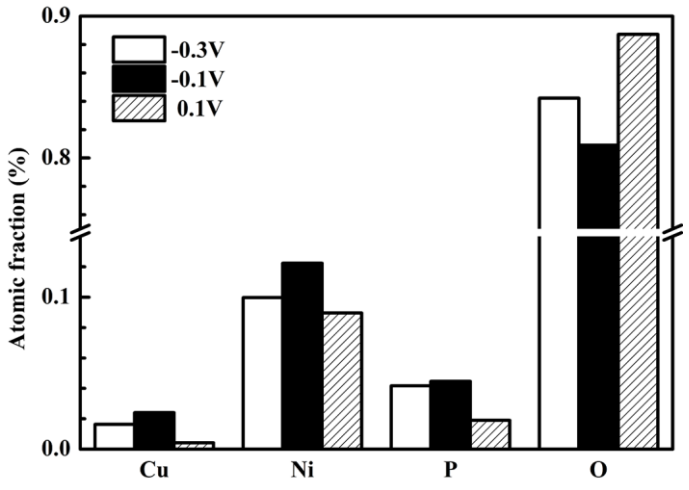

Figure 11. Fractions of the main elements in the passive films formed on amorphous Ni–Cu–P coating at –0.3, –0.1 and 0.1 V after 3600s in 10 wt.% NaOH solution.

Table 3. XPS curve fit results of Ni 2p3/2 for the amorphous Ni–Cu–P coating polarized at –0.3, –0.1 and 0.1 V

	Atomic concentration (%)			
	$Ni(OH)_2$	NiO	Ni^0	Ni^{2+}/ Ni^0
-0.3 V	7.8	0.5	1.6	5.2
-0.1 V	7.7	1.9	2.6	3.7
0.1 V	6.1	1.9	0.9	8.9

In this study, passive films formed at lower potential (–0.3 and –0.2 V) have n–type and p–type semiconductors, so it has p–n junction (a bipolar characteristic). The passive films cannot only obstruct the positive ions going out but also resist the negative ions coming in. However, the thickness of the passive film is increased with the increase of the film formation potential. The passivation films are too thin to improve their corrosion resistance significantly at lower potential. Although the passive film has only the p–type semiconductor when it is formed at higher potential (–0.1 V), the thickness of the passivation film is greatly increased, and plays the role in improving the corrosion resistance. When the passivation potential increases to a certain extent (0 and 0.1 V), the passivation film is in a unidirectional conducting state (p–type), so the protection of the passivation film on matrix is weakened. Therefore, with the increase of the applied potential, the protection of the passive film on Ni–Cu–P amorphous coating increases firstly and then exhibits an opposite trend. In a word, the protective property of passive films on Ni–Cu–P amorphous coating is combined affected by their thickness and the semiconductor type.

4. CONCLUSIONS

(1) The electroless Ni–Cu–P coating has an amorphous structure. It can form stable passive film on the surface of the coating in 10 wt. % NaOH solution, which can effectively inhibit corrosion.

(2) With the increase of the applied potential, the corrosion resistance of passive film on Ni–Cu–P amorphous coating increased firstly and then exhibits an opposite trend.

(3) Passive films formed at lower potential possess n–type and p–type bipolar semiconductors characteristics. While, the passive films formed at higher potential have only p–type semiconductor characteristics.

(4) Passive films formed on Ni–Cu–P amorphous coating is mainly composed of $Ni(OH)_2$ and NiO, as well as of a small amount of Cu_2O, CuO and $Cu(OH)_2$. In addition, the thickness of passive films on Ni–Cu–P plating was increased with the increase of passive potential.

(5) The corrosion resistance of passivation films is combined affected by their thickness and its semiconductor characteristics.

ACKNOWLEDGEMENT
This project is supported by National Natural Science Foundation of China (NO. 51271099).

References

1. G. Zhao, Y. Zou , S. Jinwen, K. Matsuda, Z. Zou and J. Chen, *Int. J. Electrochem. Sci.*,11 (2016) 140.
2. J. Georgieva and S. Armyanov, *J. Solid State Electr.*, 11 (2007) 869.
3. N. Lin, H. Zhang, J. Zou, P. Han, Y. Ma and B. Tang, *Int. J. Electrochem. Sci.*, 10 (2015) 356.
4. Y. Liu and Q. Zhao, *Appl. Surf. Sci.*, 228 (2004) 57.
5. S. Mu, W. Li and J. Du, *Electrochim. Acta*, 125 (2014) 580.
6. J. Yang, X. Zhao, J. Zhang, W. Fan, Q. Li and C. Yan, *Int. J. Electrochem. Sci.*, 10 (2015) 4523.
7. R. M. Fernández-Domene, E. Blasco-Tamarit, D. M. García-García and J. García-Antón, *Electrochim. Acta*, 95 (2013) 1.
8. C. Y. Chao, L. F. Lin and D. D. Macdonald, *Agr. Water Manage.*, 166 (2016) 1.
9. D. D. Macdonald, *Electrochim. Acta*, 56 (2011) 1761.
10. D. D. Macdonald and M. Urquidi‐Macdonald, *J. Electrochem. Soc.*, 137 (1990) 2395.
11. A. Rossi and B. Eisener, *Surf. Interface. Anal.*, 18 (1992) 499.
12. H. Tsuchiya, S. Fujimoto and T. Shibata, *J. Electroceram.*, 16 (2006) 49.
13. A. Fattah-Alhosseini, F. Soltani, F. Shirsalimi, B. Ezadi and N. Attarzadeh, *Corros. Sci.*, 53 (2011) 3186.
14. D. Macdonald and G. Englehardt, ECS Meeting, 28 (2010).
15. A. D. Paola, *Electrochim. Acta*, 34 (1989) 203.
16. S. Lee, E. Cho, S. Ahn and H. Kwon, *Electrochim. Acta*, 46 (2001) 2605.
17. R. Diegle, N. Sorensen, C. Clayton, M. Helfand and Y. Yu, *J. Electrochem. Soc.*, 135 (1988) 1085.
18. B. Hui, J. Li and L. Wang, *Wood Sci. Technol.*, 48 (2014) 961.
19. G. Liu, L. Yang, L. Wang, S. Wang, L. Chongyang and J. Wang, *Surf. Coat. Tech.*, 204 (2010) 3382.
20. J. Liu, X. Wang, Z. Tian, M. Yuan and X. Ma, *Appl. Surf. Sci.*, 356 (2015) 289.
21. P. H. Lo, W. T. Tsai, J. T. Lee and M. P. Hung, *J. Electrochem. Soc.*, 142 (1994) 91.
22. H. X. Guo, B. T. Lu and J. L. Luo, *Electrochim. Acta*, 52 (2006) 1108.
23. Z. B. Zheng, Y. G. Zheng, W. H. Sun and J. Q. Wang, *Corros. Sci.*, 82 (2014) 115.
24. M. I. Gardner, D. J. Wristers, R. Dawson, J. H. Fulford, F. N. Hause, M. W. Michael and B. T. Moore, USA patent, 5 976 956 (1999).
25. A. D. Upadhyaya, Y. W. Ok, M. Kadish, V. Upadhyaya, K. S. Ryu, M. H. Kang, A. Gupta and A. Rohatgi, : Photovoltaic Specialists Conference (PVSC), 2013 IEEE 39th. (2013) 1677.
26. G. Barral, S. Maximovitch and F. Njanjo-Eyoke, *Electrochim. Acta*, 41 (1996) 1305.
27. K. Mizuno, M. Izaki, K. Murase, T. Shinagawa, M. Chigane, M. Inaba, A. Tasaka and Y. Awakura, *J. Electrochem. Soc.*, 152 (2005) C179.
28. A. K. N. Reddy, M. G. B. Rao and J. O. M. Bockris, *Chem. Phys.*, 42 (1965) 2246.
29. B. P. Löchel and H.-H. Strehblow, *J. Electrochem. Soc.*, 131 (1984) 713.
30. M. Itoh, H. Nishihara and K. Aramaki, *J. Electrochem. Soc.*, 142 (1995) 3696.
31. A. N. Mansour and C. A. Melendres, *Surf. Sci. Spectra*, 3 (1994) 239.
32. G. Deroubaix and P. Marcus, *Surf. Interface Anal.*, 18 (1992) 39.
33. T. Robert, M. Bartel and G. Offergeld, *Surf. Sci.*, 33 (1972) 123.
34. M. Ask, J. Lausmaa and B. Kasemo, *Appl. Surf. Sci.*, 35 (1989) 283.
35. K. S. Kim and N. Winograd, *Surf. Sci.*, 43 (1974) 625.
36. R. L. I. Zeller and L. Salvati, *Corrosion (Houston); (United States)*, 50:6 (1994).
37. G. Salvago, G. Fumagalli and F. Brunella, *Surf. Coat. Tech.*, 37 (1989) 449.

38. Y. Hu, L. Yang, C. Shi and W. Tang, *Mater. Chem. Phys.*, 141 (2013) 944.
39. A. C. Lloyd, D. W. Shoesmith, N. S. Mcintyre and J. J. NoëL, *J. Electrochem. Soc.*, 150 (2003) B120.